Effect of Rare-Earth Element Substitution in Superconducting $R_3Ni_2O_7$ under Pressure

Zhiming Pan(潘志明)[1,2†], Chen Lu(卢晨)[2†], Fan Yang(杨帆)[3*], and Congjun Wu(吴从军)[2,1,4,5*]

[1]*Institute for Theoretical Sciences, Westlake University, Hangzhou 310024, China*
[2]*New Cornerstone Science Laboratory, Department of Physics, School of Science, Westlake University, Hangzhou 310024, China*
[3]*School of Physics, Beijing Institute of Technology, Beijing 100081, China*
[4]*Key Laboratory for Quantum Materials of Zhejiang Province, School of Science, Westlake University, Hangzhou 310024, China*
[5]*Institute of Natural Sciences, Westlake Institute for Advanced Study, Hangzhou 310024, China*

(Received 8 April 2024; accepted manuscript online 1 July 2024)

Recently, high temperature ($T_c \approx 80$ K) superconductivity (SC) has been discovered in $La_3Ni_2O_7$ (LNO) under pressure. This raises the question of whether the superconducting transition temperature T_c could be further enhanced under suitable conditions. One possible route for achieving higher T_c is element substitution. Similar SC could appear in the $Fmmm$ phase of rare-earth (RE) $R_3Ni_2O_7$ (RNO, R = RE element) material series under suitable pressure. The electronic properties in the RNO materials are dominated by the Ni $3d$ orbitals in the bilayer NiO_2 plane. In the strong coupling limit, the SC could be fully characterized by a bilayer single $3d_{x^2-y^2}$-orbital t–$J_\parallel$–$J_\perp$ model. With RE element substitution from La to other RE element, the lattice constant of the $Fmmm$ RNO material decreases, and the resultant electronic hopping integral increases, leading to stronger superexchanges between the $3d_{x^2-y^2}$ orbitals. Based on the slave-boson mean-field theory, we explore the pairing nature and the evolution of T_c in RNO materials under pressure. Consequently, it is found that the element substitution does not alter the pairing nature, i.e., the inter-layer s-wave pairing is always favored in the superconducting RNO under pressure. However, the T_c increases from La to Sm, and a nearly doubled T_c could be realized in SmNO under pressure. This work provides evidence for possible higher T_c $R_3Ni_2O_7$ materials, which may be realized in further experiments.

DOI: 10.1088/0256-307X/41/8/087401

The recent discovered high-temperature superconductivity in $La_3Ni_2O_7$ (LNO) under pressure[1] has attracted significant interests experimentally[2–7] and theoretically.[8–45] The signature of the superconducting transition temperature T_c is approximately 80 K under pressures exceeding 14 GPa,[1] which manifests as a new platform of studying high-T_c superconductor other than cuprates.[46,47]

The basic ingredient for the electronic properties in LNO is the two E_g orbitals of $Ni^{2.5+}$ in the bilayer NiO_2 planes,[1] sharing a similar lattice structure with cuprates. On average, each $Ni^{2.5+}$ ion is half-filled in its $3d_{z^2}$ orbital and quarter-filled in its $3d_{x^2-y^2}$ orbital. The spin alignments in the two E_g orbitals are strongly entangled together due to Hund's rule. The $3d_{z^2}$ electrons can hop between the two NiO_2 layers through intermediate O $2p_z$ orbitals, while the $3d_{x^2-y^2}$ electrons primarily hop within the layers. The physical dopings of the two E_g orbitals can deviate from the above bare values, due to the self-doped effect from hybridization between E_g orbitals[26,28] or hole doping on the O $2p$ orbitals.[17]

Taken into account Hund's rule, we have proposed an effective bilayer single-$3d_{x^2-y^2}$ orbital t–$J_\parallel$–$J_\perp$ model in the strong coupling limit as the minimal model for high-T_c superconductivity in LNO.[21] Each NiO_2 layer is described by a conventional t–$J_\parallel$ model with nearest-neighbor intra-layer antiferromagnetic (AFM) spin exchange $J_\parallel$. The two NiO_2 layers are coupled through an effective inter-layer AFM spin exchange $J_\perp$ between $3d_{x^2-y^2}$ electrons in the two layers, which is generated by integrating out the $3d_{z^2}$ orbital degrees of freedom under strong Hund's coupling. The superconducting transition temperature could be dramatically enhanced when the inter-layer coupling $J_\perp$ is larger than the intra-layer one.[21] This type of bilayer t–J model has already been explored in multilayer cuprates[48–52] and may be realized in ultracold atoms.[53–55] Most of these works focus on the theoretical side with different physical parameter regime.[48–59] In particular, the strong interlayer coupling $J_\perp$ in LNO plays an important role in achieving high T_c,[21] while such strong $J_\perp$ is hard to realize in multilayer cuprates.

Element substitution is an important chemical approach to increasing the superconducting transition temperature. Replacing the La element with other rare-earth (RE) elements can influence the crystal and electronic structure of the materials. Moreover, under suitable pressure, $R_3Ni_2O_7$ (RNO, R = RE elements) material series could undergo a similar structure transition to the $Fmmm$

†These authors contributed equally to this work.
*Corresponding authors. Email: yangfan_blg@bit.edu.cn; wucongjun@westlake.edu.cn
© 2024 Chinese Physical Society and IOP Publishing Ltd

phase as LNO. Previous first-principle density functional theory (DFT) studies reveal the electronic structure for such RNO series.[28] The physical parameters during the structural transition to the *Fmmm* phase under suitable pressure are simulated.[28] Their results show that the hopping integrals could be enhanced from LNO to RNO, depending on the rare-earth element and the pressure. Weak coupling analysis based on random phase approximation (RPA) predicts that the pairing strength is reduced from La to Sm, and the superconducting transition temperature T_c decreases simultaneously.[28] This calculation might suggest that LNO already has the highest T_c in the RNO material series.

The situation could be reversed in the strong coupling scenario, where effect of strong superexchange strength $J_\perp$ is relevant to the high-T_c superconductivity.[21] Based on the hopping integrals from the DFT calculations,[28] the effective AFM couplings $J_\perp$ and $J_\parallel$ increase from La to Sm under suitable pressure. All the relevant energy scales could increase, opening up the possibility of realizing high T_c in RNO materials. Previous calculations have already seen that strong super-exchange $J_\perp$ could enhance T_c, leading to the high-T_c observed in the LNO experiment.[21] These observations suggest potential increased T_c under elements substitution.

In this work, we study the effect of RE element substitution in RNO materials under pressure based on the effective bilayer single $3d_{x^2-y^2}$-orbital t–$J_\parallel$–$J_\perp$ model.[21] We first obtain the effective AFM spin exchange $J_\perp$ and $J_\parallel$ for the relevant conditions from the DFT calculation.[28] Then, we apply the slave-boson mean field analysis[60,61] for the bilayer t–J model within these physical parameters. The superconducting pairing gaps and transition temperatures T_c are numerically calculated. Our results suggest that element substitution does not change the pairing nature of high-T_c superconductivity in RNO under pressure, i.e., the inter-layer s-wave pairing. Nevertheless, the predicted T_c could be strongly enhanced in rare-earth RNO under pressure in this strong coupling scenario, and particularly from La to Sm, T_c nearly doubles. This work provides a possible route for enhancing T_c and appeals for experimental verification.

Effective Bilayer Model. In the double-layered Ruddlesden–Popper $R_3Ni_2O_7$ material, electronic properties are determined by the bilayer NiO_2 planes. DFT calculations[1,28,62] indicate that the relevant physical degrees of freedom near the Fermi surface come from the two E_g orbitals in $Ni^{2.5+}$ ions, where $3d_{z^2}$ orbital is half-filled and $3d_{x^2-y^2}$ orbital is quarter-filled. The inter-layer hopping $t_{zz}^{\perp}$ between the $3d_{z^2}$ orbitals and the intra-layer hopping $t_{xx}^{\parallel}$ between the $3d_{x^2-y^2}$ orbitals dominate the electron mobile process. In the strong coupling limit with large Hubbard-U, an effective inter-layer spin superexchange for $3d_{z^2}$ orbitals and an intra-layer one for $3d_{x^2-y^2}$ orbitals are generated, which are approximately given by

$$J_\perp = \frac{4t_{zz}^{\perp 2}}{U}, \quad J_\parallel = \frac{4t_{xx}^{\parallel 2}}{U}. \tag{1}$$

Furthermore, $J_\perp$ is larger than $J_\parallel$ due to the larger inter-layer hopping of $3d_{z^2}$ orbitals.

The relevant physics of possible high-T_c superconductivity in RNO under pressure can be characterized by a bilayer E_g-orbital t–J–J_H model,

$$\begin{aligned} H = & -t_{xx}^{\parallel} \sum_{\langle i,j\rangle\alpha\sigma} (d^{\dagger}_{x^2 i\alpha\sigma} d_{x^2 j\alpha\sigma} + \text{h.c.}) \\ & + J_\parallel \sum_{\langle i,j\rangle\alpha} \boldsymbol{S}_{x^2 i\alpha} \cdot \boldsymbol{S}_{x^2 j\alpha} \\ & + J_\perp \sum_i \boldsymbol{S}_{z^2 i1} \cdot \boldsymbol{S}_{z^2 i2} - J_H \sum_{i\alpha} \boldsymbol{S}_{x^2 i\alpha} \cdot \boldsymbol{S}_{z^2 i\alpha}, \end{aligned} \tag{2}$$

where $d^{\dagger}_{x^2 i\alpha\sigma}$ is the electron creation operator for the $3d_{x^2-y^2}$ orbital at lattice site i, $\alpha = 1, 2$ represents the layer index for the NiO plane, and $\sigma = \uparrow, \downarrow$ is the spin index. $\boldsymbol{S}_{x^2 i\alpha} = \frac{1}{2} d^{\dagger}_{x^2 i\alpha}[\boldsymbol{\sigma}] d_{x^2 i\alpha}$ is the spin operator for the $3d_{x^2-y^2}$ electron, with Pauli matrix $\boldsymbol{\sigma} = (\sigma_x, \sigma_y, \sigma_z)$. The summation $\sum_{\langle i,j\rangle}$ takes over all the nearest neighboring sites $\langle i, j\rangle$ within the NiO plane. $S_{z^2 i\alpha}$ is the spin operator for the localized $3d_{z^2}$ orbital. The two orbitals interact through the strong on-site Hund's coupling J_H. Under rare-earth element substitution, the magnitude of Hund's coupling remains relatively stable, significantly exceeding the values of $J_\parallel$ and $J_\perp$. Within the regime of strong Hund's coupling, the specific value of this large J_H does not substantially influence the physics.

The effective minimal model under strong Hund's coupling is a bilayer t–$J_\parallel$–$J_\perp$ model for the single $3d_{x^2-y^2}$ orbital.[21] The strong Hund's coupling binds the spins of $3d_{x^2-y^2}$ and $3d_{z^2}$ orbitals into a spin-triplet state. The inter-layer $3d_{z^2}$ spin exchange $J_\perp$ is transmitted to the $3d_{x^2-y^2}$ spins, generating an effective inter-layer spin exchange $J_\perp$ between the $3d_{x^2-y^2}$ spins. Integrating out the $3d_{z^2}$ degrees of freedom under strong Hund's coupling ($J_H \gg J_\perp$), the two-orbital model Eq. (2) could be further reduced to a bilayer single $3d_{x^2-y^2}$-orbital model,

$$\begin{aligned} H = & -t_{xx}^{\parallel} \sum_{\langle i,j\rangle\alpha\sigma} (d^{\dagger}_{x^2 i\alpha\sigma} d_{x^2 j\alpha\sigma} + \text{h.c.}) \\ & - t_{xx}^{\perp} \sum_{i\sigma} (d^{\dagger}_{x^2 i1\sigma} d_{x^2 i2\sigma} + \text{h.c.}) \\ & + J_\parallel \sum_{\langle i,j\rangle\alpha} \boldsymbol{S}_{x^2 i\alpha} \cdot \boldsymbol{S}_{x^2 j\alpha} + J_\perp \sum_i \boldsymbol{S}_{x^2 i1} \cdot \boldsymbol{S}_{x^2 i2}, \end{aligned} \tag{3}$$

with intra-layer nearest-neighbor AFM spin exchanges $J_\parallel$ and inter-layer one $J_\perp$, as depicted in Fig. 1. A small inter-layer hopping $t_{xx}^{\perp}$ is added, which can fix the relative phases between the pairings of the two layers. In the reduced model, the hidden $3d_{z^2}$ orbital acts as an intermediate bridge for the inter-layer coupling $J_\perp$ between $3d_{x^2-y^2}$ orbitals. It also accounts for the self-doping effect in the $3d_{x^2-y^2}$ orbital.[26,28]

The filling level x (or doping level $\delta = 1 - 2x$) of the $3d_{x^2-y^2}$ orbital deviates from quarter filling due to the hybridization between the two E_g orbitals. Although C_4 rotation symmetry around the z-axis forbids the on-site hybridization between the $3d_{z^2}$ and $3d_{x^2-y^2}$ orbital, symmetry arguments still allow for finite hybridization between neighbor sites. In DFT calculation,[8,28] this nearest-neighbor hybridization between $3d_{z^2}$ and $3d_{x^2-y^2}$ orbitals has been shown to be comparable to the nearest-neighbor hopping in the RNO materials under pressure. The mixing of the two orbitals leads to bonding or anti-bonding

states. Moreover, an effective intra-layer hopping process mediated by the $3d_{x^2-y^2}$ orbital could be generated for the $3d_{z^2}$ orbital. The averaged densities of the $3d_{z^2}$ and $3d_{x^2-y^2}$ orbitals deviate from their bare values due to density fluctuations.

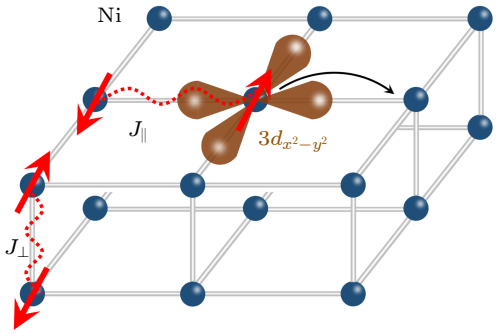

Fig. 1. Schematic diagram for the effective single $3d_{x^2-y^2}$ orbital bilayer t–$J_\parallel$–$J_\perp$ model. Each layer is comprised by a conventional intra-layer t–$J_\parallel$ model, while the two layers interact through an inter-layer spin exchange $J_\perp$.

For the RE element substitution from La to Sm in RNO under pressure, DFT calculations show that the $3d_{x^2-y^2}$ maintains a filling level of approximately $x \approx 0.3$.[28] Meanwhile, the filling of $3d_{z^2}$ orbital is close to 0.45, which does not deviate significantly from half-filling, justifying the nearly half-filled nature of this orbital. $3d_{z^2}$ orbitals could be considered as localized spins degree of freedom, which are integrated out in the effective single-orbital model.

Slave Boson Mean Field Theory. In the slave boson mean field theory,[60,61] the $3d_{x^2-y^2}$-orbital electron operator is represented as $d^\dagger_{x^2i\alpha\sigma} = f^\dagger_{i\alpha\sigma} b_{i\alpha}$, where $f^\dagger_{i\alpha\sigma}$ is the spinon creation operator and $b_{i\alpha}$ is the holon annihilation operator. The spin superexchange can be decoupled in the hopping and pairing channels. For the inter-layer case, we have

$$\begin{aligned} & J_\perp \boldsymbol{S}_{x^2i1} \cdot \boldsymbol{S}_{x^2i2} \\ = & -\left[\chi_{i\perp}(f^\dagger_{i1\uparrow} f_{i2\uparrow} + f^\dagger_{i1\downarrow} f_{i2\downarrow}) + \text{h.c.} - \frac{8|\chi_{i\perp}|^2}{3J_\perp}\right] \\ & -\left[\Delta_{i\perp}(f^\dagger_{i1\uparrow} f^\dagger_{i2\downarrow} - f^\dagger_{i1\downarrow} f^\dagger_{i2\uparrow}) + \text{h.c.} - \frac{8|\Delta_{i\perp}|^2}{3J_\perp}\right]. \end{aligned} \tag{4}$$

A similar decomposition applies to the intra-layer superexchange $J_\parallel$. In the mean-field ansatz, the hopping and pairing order parameters are represented by their mean-field values,[21]

$$\begin{aligned} \chi^{(\alpha)}_{ij} &= \frac{3}{8} J_\parallel \langle f^\dagger_{j\alpha\uparrow} f_{i\alpha\uparrow} + f^\dagger_{j\alpha\downarrow} f_{i\alpha\downarrow}\rangle \equiv \chi^{(\alpha)}_{j-i}, \\ \Delta^{(\alpha)}_{ij} &= \frac{3}{8} J_\parallel \langle f_{j\alpha\downarrow} f_{i\alpha\uparrow} - f_{j\alpha\uparrow} f_{i\alpha\downarrow}\rangle \equiv \Delta^{(\alpha)}_{j-i}, \\ \chi_{i\perp} &= \frac{3}{8} J_\perp \langle f^\dagger_{i2\uparrow} f_{i1\uparrow} + f^\dagger_{i2\downarrow} f_{i1\downarrow}\rangle \equiv \chi_\perp, \\ \Delta_{i\perp} &= \frac{3}{8} J_\perp \langle f_{i2\downarrow} f_{i1\uparrow} - f_{i2\uparrow} f_{i1\downarrow}\rangle \equiv \Delta_\perp. \end{aligned} \tag{5}$$

The holons condense at low temperatures, and the holon operator can be replaced by its condensation density below the condensation temperature, $b_{i\alpha} \sim b^\dagger_{i\alpha} \sim \sqrt{\delta} = \sqrt{1-2x}$.

The superconducting state is realized when the spinons are paired, and the holons are condensed.[60] There are two typical temperature scales: T_{BEC} for holon condensation, and T_{pair} for spinon pairing. The doping dependence of these scales differs from each other. T_{BEC} increases almost linearly with the doping level δ increasing, and is typical much larger than T_{pair} near quarter filling. The spinon pairing temperature sets the onset of superconductivity, and the superconducting transition temperature is given by $T_c = T_{\text{pair}}$. Due to the stronger inter-layer exchange, T_c would be enhanced in RNO series under pressure.

RE Element Substitution. Under the RE element substitution from La to Sm, the lattice constants decrease, and the overlaps of neighboring electronic orbitals increase in RNO $Fmmm$ phase under suitable pressure. As a result, both the intra-layer $3d_{x^2-y^2}$ orbital hopping and inter-layer $3d_{z^2}$ hopping will gradually increase. In contrary, the on-site Hubbard U interaction does not change much. We adopt the hopping integral strengths and Hubbard $U \simeq 4$ eV from the DFT calculations in Ref. [28] for the RNO series under pressure, where possible superconductivity could be realized. The effective inter-layer and intra-layer AFM spin superexchange are obtained from Eq. (1), as depicted in Fig. (2). $J_\perp$ and $J_\parallel$ increase from La to Sm, while their ratio remains nearly unchanged, $J_\perp/J_\parallel \approx 1.65$–$1.70$. Notably, for element substitution of Pm or Sm in RNO under pressure, the hopping strength and spin exchange become significantly stronger. The relevant energy scales are enhanced simultaneously, opening up the possibility of increasing T_c.

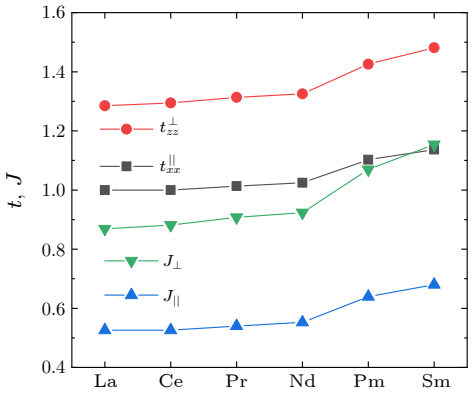

Fig. 2. Relevant hopping integrals and effective spin exchange for different RE elements from La to Sm in RNO $Fmmm$ phase under pressure. From La to Sm, the inter-layer $3d_{z^2}$ hopping $t^\perp_{zz}$ and intra-layer $3d_{x^2-y^2}$ hopping $t^\parallel_{xx}$ both gradually increase.[28] The effective inter-layer $3d_{z^2}$ spin exchange $J_\perp$ and intra-layer $3d_{x^2-y^2}$ spin exchange $J_\parallel$ follow the similar tendency. We have set $t^\parallel_{xx} = 1$ for LNO as the unit.

In the relevant parameter regime, an inter-layer s-wave pairing with high T_c is deduced for RNO materials under pressure, similar to LNO.[21] The superconducting state is dominated by the inter-layer $3d_{x^2-y^2}$ orbital s-wave pairing $\Delta_\perp$, where the intra-layer pairing $\Delta^{(\alpha)}_\mu$ ($\mu = x$, y and $\alpha = 1$, 2) nearly vanishes. This strong inter-layer pairing is a direct consequence of the large inter-layer superexchange $J_\perp$ compared to the intra-layer one $J_\parallel$. In RNO materials, with RE elements substitution from La to Sm under pressure, the inter-layer pairings $\Delta_\perp$ increase as the fill-

ing level increases, as depicted in Fig. 3(a). The enhanced inter-layer pairings indicate possible higher pairing temperatures.

The strong inter-layer superexchange $J_\perp$ significantly enhances the transition temperature, leading to possible high T_c superconductivity in the RNO materials under pressure. The superconducting T_c for RNO is numerically estimated as a function of the filling level x, as depicted in Fig. 3(b). As x increases from quarter filling ($x = 0.25$), the transition temperature tends to increasing monotonically. Additionally, with RE element substitution from La to Sm under pressure, the transition temperature T_c is enhanced for the same filling level and experiences a significant jump for Pm or Sm. This strong enhancement in T_c results from the increased energy scales for Pm and Sm element, as clearly seen in Fig. (2). Moreover, the ratio between the pairing gap $\Delta_\perp$ and superconducting T_c is approximately $\Delta_\perp/T_c \approx 0.4/0.25 = 1.6$, which is quantitatively consistent with the prediction of BCS-type theory.

At the physical filling level $x \approx 0.3$, the superconducting T_c nearly doubles from La to Sm element under suitable pressure. It is expected that $Sm_3Ni_2O_7$ is the potential optimal material with the largest T_c in the RNO material series. Furthermore, a slight increase in the filling magnitude x from La to Sm element is observed.[28] Consequently, as illustrated in Fig. 3, if x is increased through element substitution, the critical temperature could be further enhanced.

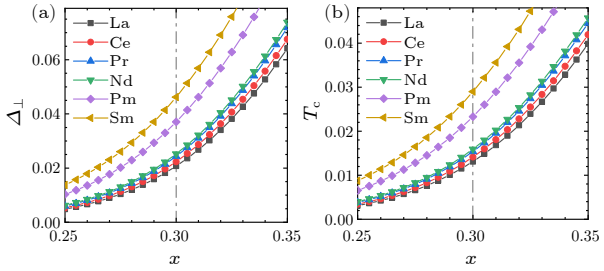

Fig. 3. (a) Inter-layer pairing gap $\Delta_\perp$ versus filling level x under element substitution for $R_3Ni_2O_7$ (R = RE element from La to Sm) $Fmmm$ phase under pressure. The place of physical filling $x \approx 0.3$ is shown in a dashed-dotted line. The superconducting gap increases as the filling level grows. (b) Superconducting transition temperature T_c versus filling level x under element substitution for RNO $Fmmm$ phase. From La to Sm, the pairing strength $\Delta_\perp$ and the superconducting T_c in RNO series under pressure increase simultaneously.

Discussion. In the RNO materials, pressure induced structural transition to the $Fmmm$ phase opens up the possibility of high-T_c superconductivity as in LNO. Numerical simulations show that $Sm_3Ni_2O_7$ could exhibit the largest superconducting T_c. The scenario proposed here differs from previous weak coupling analysis based on RPA,[28] where superconductivity is dominated by the $3d_{z^2}$ orbital.

In weak-coupling BCS-type theories, T_c is approximately given by $T_c \propto \exp[-1/(gN_F)]$, where N_F is the density of state near the Fermi level and g is the effective interaction strength. For the $3d_{z^2}$ orbital, increasing the hopping integral through element substitution leads to a reduction in N_F. Furthermore, within the framework of RPA, the effective interaction strength is proportional to the bare susceptibility, which is inversely related to the energy levels. As the hopping integral increases, the energy level decreases, leading to a reduction in the bare susceptibility. Consequently, in the weak coupling theory, T_c would decrease with element substitution from La to Sm.[28]

For LNO material under pressure, it is generally believed that the physical Hubbard interaction strength U of the system is approximately 4–5 eV,[62] which would also hold true for RNO series. However, due to methodological limitations, the weakly correlated RPA method employs a U value of only 0.8 eV, which significantly underestimates the actual interaction strength.[28] In contrast, the strongly correlated t–$J_\parallel$–$J_\perp$ model utilizes an interaction strength U of approximately 4 eV and considers the large-U limit. The effective interaction strength is tied to the superexchange interaction $J_\perp$, which scales approximately with t^2. Consequently, within the framework of strong coupling theory, the critical temperature T_c is predicted to increase with element substitution from La to Sm, reflecting the enhanced superexchange interactions in these substituted systems.

As we emphasized in previous work[21] and further confirm in this work, the high-T_c superconductivity in RNO candidates under pressure is driven by the strong inter-layer spin superexchange $J_\perp$ for the $3d_{x^2-y^2}$ orbitals. The inter-layer s-wave superconducting pairing in the $3d_{x^2-y^2}$ orbital is favored in the relevant parameter regime, with intra-layer hopping serving as the mobile engine. This situation is distinct from the d-wave pairing in the single-layer cuprate[60] and multilayer cuprates where the inter-layer exchange $J_\perp$ is naturally smaller than $J_\parallel$.[48–52] The wavefunctions of $3d_{x^2-y^2}$ orbital lie nearly within the plane, resulting in small interlayer overlap between $3d_{x^2-y^2}$ orbitals. The strong $J_\perp > J_\parallel$ is hard to be directly generated from the much smaller inter-layer hopping of single $3d_{x^2-y^2}$ orbitals compared to the intra-layer one. In RNO materials under pressure, the inter-layer overlap of $3d_{z^2}$ orbital wavefunctions allows for strong inter-layer hopping. Strong $J_\perp$ can be realized for $3d_{z^2}$ orbitals and is further transmitted to $3d_{x^2-y^2}$ orbitals under strong Hund's coupling.

Although we focus on the reduced single $3d_{x^2-y^2}$ orbital model, the effect of hidden $3d_{z^2}$ degrees of freedom plays an important role. Notably, $3d_{z^2}$ electrons are nearly localized within the plane, and strong inter-layer hopping induces strong inter-layer super-exchange $J_\perp$. There are also inter-layer pairings for the almost half-filled $3d_{z^2}$ orbitals. However, these pairings are nearly localized. The $3d_{z^2}$ orbital is nearly half-filled, and its holon condensation temperature is quite low due to its low density. Consequently, $3d_{z^2}$ orbitals do not directly contribute to the superconducting transport behavior. On the contrary, Hund's rule combines the two E_g orbitals into the spin-triplet states, inducing effective strong inter-layer couplings $J_\perp$ between $3d_{x^2-y^2}$ orbitals.

While the simplified single orbital model captures the most relevant physics of the superconducting LNO material under pressure,[21] further theoretical work and exper-

imental exploration are necessary for understanding the interplay between $3d_{x^2-y^2}$ and $3d_{z^2}$ orbitals. Moreover, the nature of the superconductivity in the $3d_{x^2-y^2}$ and $3d_{z^2}$ orbitals is different. A comprehensive analysis that takes into account both degrees of freedom will be helpful. Possible chemical doping approach may alter the superconducting behavior and increase the T_c. We will leave these problems in the further works.[45]

In summary, we focus on the effect of RE element substitution on high T_c superconductivity in RNO materials under pressure based on the strong coupling bilayer single $3d_{x^2-y^2}$ orbital t–$J_\parallel$–$J_\perp$ model. For RE element from La to Sm under pressure, the effective inter-layer and intra-layer spin superexchange increases as the relevant hopping integrals grow. At the relevant filling level, the superconducting T_c is enhanced in element-substituted RNO under pressure. Strikingly, T_c nearly doubles from LNO to SmNO under pressure, which might be experimentally realized in the future. This work suggests that RE element substitution in *Fmmm* RNO materials under pressure is an important approach to enhance the superconducting T_c, appealing for further experimental verification.

Acknowledgments. This work was supported by the National Natural Science Foundation of China (Grant Nos. 12234016, 12174317, and 12074031), and the New Cornerstone Science Foundation.

References

[1] Sun H, Huo M, Hu X, Li J, Liu Z, Han Y, Tang L, Mao Z, Yang P, Wang B, Cheng J, Yao D X, Zhang G M, and Wang M 2023 *Nature* **621** 493
[2] Liu Z, Huo M W, Li J, Li Q, Liu Y C, Dai Y M, Zhou X X, Hao J H, Lu Y, Wang M, and Wen H H 2023 arXiv:2307.02950 [cond-mat.supr-con]
[3] Hou J, Yang P T, Liu Z Y, Li J Y, Shan P F, Ma L, Wang G, Wang N N, Guo H Z, Sun J P, Uwatoko Y, Wang M, Zhang G M, Wang B S, and Cheng J G 2023 *Chin. Phys. Lett.* **40** 117302
[4] Zhang Y N, Su D J, Huang Y N, Sun H L, Huo M W, Shan Z Y, Ye K X, Yang Z H, Li R, Smidman M, Wang M, Jiao L, and Yuan H Q 2023 arXiv:2307.14819 [cond-mat.supr-con]
[5] Yang J G, Sun H L, Hu X W *et al.* 2024 *Nat. Commun.* **15** 4373
[6] Zhang M, Pei C, Wang Q, Zhao Y, Li C, Cao W, Zhu S, Wu J, and Qi Y 2024 *J. Mater. Sci. Technol.* **185** 147
[7] Wang G, Wang N N, Shen X L *et al.* 2024 *Phys. Rev. X* **14** 011040
[8] Luo Z, Hu X, Wang M, Wú W, and Yao D X 2023 *Phys. Rev. Lett.* **131** 126001
[9] Zhang Y, Lin L F, Moreo A, and Dagotto E 2023 *Phys. Rev. B* **108** L180510
[10] Yang Q G, Wang D, and Wang Q H 2023 *Phys. Rev. B* **108** L140505
[11] Lechermann F, Gondolf J, Bötzel S, and Eremin I M 2023 *Phys. Rev. B* **108** L201121
[12] Sakakibara H, Kitamine N, Ochi M, and Kuroki K 2024 *Phys. Rev. Lett.* **132** 106002
[13] Gu Y H, Le C C, Yang Z S, Wu X X, and Hu J P 2023 arXiv:2306.07275 [cond-mat.supr-con]
[14] Shen Y, Qin M, and Zhang G M 2023 *Chin. Phys. Lett.* **40** 127401
[15] Christiansson V, Petocchi F, and Werner P 2023 *Phys. Rev. Lett.* **131** 206501
[16] Shilenko D A and Leonov I V 2023 *Phys. Rev. B* **108** 125105
[17] Wú W, Luo Z, Yao D X, and Wang M 2024 *Sci. China Phys. Mech. Astron.* **67** 117402
[18] Cao Y and Yang Y F 2024 *Phys. Rev. B* **109** L081105
[19] Chen X J, Jiang P H, Li J, Zhong Z C, and Lu Y 2023 arXiv:2307.07154 [cond-mat.supr-con]
[20] Liu Y B, Mei J W, Ye F, Chen W Q, and Yang F 2023 *Phys. Rev. Lett.* **131** 236002
[21] Lu C, Pan Z, Yang F, and Wu C 2024 *Phys. Rev. Lett.* **132** 146002
[22] Zhang Y, Lin L F, Moreo A, Maier T A, and Dagotto E 2024 *Nat. Commun.* **15** 2470
[23] Oh H and Zhang Y H 2023 *Phys. Rev. B* **108** 174511
[24] Liao Z G, Chen L, Duan G J, Wang Y M, Liu C L, Yu R, and Si Q M 2023 arXiv:2307.16697 [cond-mat.supr-con]
[25] Qu X Z, Qu D W, Chen J, Wu C, Yang F, Li W, and Su G 2024 *Phys. Rev. Lett.* **132** 036502
[26] Yang Y F, Zhang G M, and Zhang F C 2023 *Phys. Rev. B* **108** L201108
[27] Jiang K, Wang Z, and Zhang F C 2024 *Chin. Phys. Lett.* **41** 017402
[28] Zhang Y, Lin L F, Moreo A, Maier T A, and Dagotto E 2023 *Phys. Rev. B* **108** 165141
[29] Huang J, Wang Z D, and Zhou T 2023 *Phys. Rev. B* **108** 174501
[30] Qin Q and Yang Y F 2023 *Phys. Rev. B* **108** L140504
[31] Tian Y H, Chen Y, Wang J M, He R Q, and Lu Z Y 2024 *Phys. Rev. B* **109** 165154
[32] Lu D C, Li M, Zeng Z Y, Hou W D, Wang J, Yang F, and You Y Z 2023 arXiv:2308.11195 [cond-mat.str-el]
[33] Jiang R, Hou J, Fan Z, Lang Z J, and Ku W 2024 *Phys. Rev. Lett.* **132** 126503
[34] Kitamine N, Ochi M, and Kuroki K 2023 arXiv:2308.12750 [cond-mat.supr-con]
[35] Luo Z H, Lv B, Wang M, Wú W, and Yao D X 2023 arXiv:2308.16564 [cond-mat.str-el]
[36] Zhang J X, Zhang H K, You Y Z, and Weng Z Y 2023 arXiv:2309.05726 [cond-mat.str-el]
[37] Sakakibara H, Ochi M, Nagata H, Ueki Y, Sakurai H, Matsumoto R, Terashima K, Hirose K, Ohta H, Kato M, Takano Y, and Kuroki K 2024 *Phys. Rev. B* **109** 144511
[38] Lange H, Homeier L, Demler E, Schollwöck U, Bohrdt A, and Grusdt F 2023 arXiv:2309.13040 [cond-mat.str-el]
[39] Geisler B, Hamlin J J, Stewart G R, Hennig R G, and Hirschfeld P J 2024 *npj Quantum Mater.* **9** 38
[40] Yang H, Oh H, and Zhang Y H 2023 arXiv:2309.15095 [cond-mat.str-el]
[41] Rhodes L C and Wahl P 2024 *Phys. Rev. Mater.* **8** 044801
[42] Lange H, Homeier L, Demler E, Schollwöck U, Grusdt F, and Bohrdt A 2023 arXiv:2309.15843 [cond-mat.str-el]
[43] LaBollita H, Pardo V, Norman M R, and Botana A S 2023 arXiv:2309.17279 [cond-mat.str-el]
[44] Kumar U, Melnick C, and Kotliar G 2023 arXiv:2310.00983 [cond-mat.str-el]
[45] Lu C, Pan Z M, Yang F, and Wu C J 2023 arXiv:2310.02915 [cond-mat.str-el]
[46] Bednorz J G and Müller K A 1986 *Z. Phys. B* **64** 189
[47] Proust C and Taillefer L 2019 *Annu. Rev. Condens. Matter Phys.* **10** 409
[48] Ubbens M U and Lee P A 1994 *Phys. Rev. B* **50** 438
[49] Kuboki K and Lee P A 1995 *J. Phys. Soc. Jpn.* **64** 3179
[50] Maly J, Liu D Z, and Levin K 1996 *Phys. Rev. B* **53** 6786
[51] Nazarenko A and Dagotto E 1996 *Phys. Rev. B* **54** 13158
[52] Medhi A, Basu S, and Kadolkar C 2009 *Eur. Phys. J. B* **72** 583
[53] Bohrdt A, Homeier L, Reinmoser C, Demler E, and Grusdt F 2021 *Ann. Phys.* **435** 168651
[54] Bohrdt A, Homeier L, Bloch I, Demler E, and Grusdt F 2022 *Nat. Phys.* **18** 651
[55] Hirthe S, Chalopin T, Bourgund D, Bojović P, Bohrdt A, Demler E, Grusdt F, Bloch I, and Hilker T A 2023 *Nature* **613** 463
[56] Eder R, Ohta Y, and Maekawa S 1995 *Phys. Rev. B* **52** 7708
[57] Vojta M and Becker K W 1999 *Phys. Rev. B* **60** 15201
[58] Zhao H and Engelbrecht J R 2005 *Phys. Rev. B* **71** 054508
[59] Zegrodnik M and Spałek J 2017 *Phys. Rev. B* **95** 024507
[60] Kotliar G and Liu J 1988 *Phys. Rev. B* **38** 5142
[61] Lee P A, Nagaosa N, and Wen X G 2006 *Rev. Mod. Phys.* **78** 17
[62] Pardo V and Pickett W E 2011 *Phys. Rev. B* **83** 245128